Emission of 3914-Å N_2^+ radiation from charge-transfer excitation

James M. Hoffman, Grant J. Lockwood, and Glenn H. Miller
Sandia National Laboratories, Albuquerque, New Mexico 87185
(Received 3 February 1981)

Using various projectile ions incident on an N_2 gas target, we have determined cross sections for the N_2^+ 3914-Å emission in coincidence with charge transfer from N_2 molecules to the projectiles. Ions of H and the inert gases, each in the energy range 10 to 100 keV, were used. As in charge transfer in which target and projectile are left in the ground state, the velocity at which the maximum cross section occurs increases as the magnitude of the potential energy change increases. Unlike the ground-state case, the value of the cross section at a fixed velocity is significantly greater for an exothermic reaction than for an endothermic reaction having the same magnitude of ΔE.

I. INTRODUCTION

In this paper we have studied a particular type of collision between energetic ions and target molecules. These collisions are characterized by electron transfer from the target to the projectile such that the residual molecular ion is left in an electronically excited state. These events were studied by the detection of coincidence between the resulting target radiation and the neutralized projectile. The molecular ion radiation examined was the 3914-Å band from the N_2^+ first negative system. Projectile ions employed were H^+ and singly charged ions of the inert gases.

These measurements are of interest in connection with phenomenology of the upper atmosphere. Furthermore, they provide basic information concerning atomic and molecular collisions. When energetic ions collide with atoms or molecules, excited target ions may be produced in a single collision by two processes. The first is an ionizing event in which the target is left in an excited state. This is represented by

$$A^+ + B \rightarrow A^+ + (B^+)^* + e\,,$$

where A and B are the projectile and target species, respectively. The minimum energy required for this process does not depend on the projectile ionization potential but is just the energy difference between the state of the residual target ion and the initial state of the target. The second process is electron transfer from the target to the projectile with the target being left in the excited state. For this process we have

$$A^+ + B \rightarrow A + (B^+)^*.$$

The minimum energy required for this charge-transfer-excitation process (CTE) is that required for the first process less the ionization energy of the projectile ion. We designate the negative of this minimum energy by ΔE. Table I gives the value of ΔE for the $B\,^2\Sigma(v'=0)$ state of N_2^+ for each projectile used. Also shown is E_i, the ionization energy of the projectile.[1] It has been assumed that the projectile is in the ground state both prior to and following the collision.

As in the case of charge transfer in which the residual target ion is left in the ground state, one might expect that the cross section for CTE will have an energy dependence strongly related to ΔE. Further, there may be some generalization analagous to the adiabatic criterion. This criterion states that the charge-transfer cross section between ground states should be small unless the projectile velocity is of the order of

$$\frac{a|\Delta E|}{h}\,,$$

where h is Planck's constant and a is an impact parameter.[2]

There are numerous measurements of the total emission cross sections for the 3914-Å band in the literature.[3] These measurements cover a variety of projectiles and energies. Inferences as to the relative importance of the two contributory processes based on total cross sections are unreliable, however. In the cases of F^+ and Ne^+ the energy dependence of the total emission cross section closely resembles that of the total charge-transfer cross section, while for Na^+ there is little similarity.[4] Such comparisons are at best inconclusive, and only a direct measurement of

TABLE I. Energy defect ΔE for charge-transfer excitation and first ionization potential of the projectile.

Projectile	ΔE (eV)	E_i (eV)
H	−5.15	13.60
He	+5.84	24.59
Ne	+2.81	21.56
Ar	−2.99	15.76
Kr	−4.75	14.00
Xe	−6.62	12.13

 © 1981 The American Physical Society

the cross section for one of the two processes will provide information as to their relative contributions.

There have been several measurements of emission by the projectile after capture of an electron into an excited state.[3] In such cases the reaction leading to the excited state is unambiguous, since the particular projectile radiation cannot be produced by any other single-collision process. Very little data are available for CTE of the target, however. Wehrenberg and Clark[5] used a coincidence technique to measure CTE cross sections for the 3914-Å N_2^+ band for incident protons in the energy range 5–65 keV. Their measurements were not absolute, but cross sections were obtained by normalizing relative cross sections obtained from their total photon counting rates to the total emission cross sections of DeHeer and Aarts.[6] They found that the contribution of CTE to the total emission dropped from about 90% at 10 keV to about 40% at 60 keV. The work of Young, Murray, and Sheridan[7] is also related to the present work. They made photon-photon coincidence measurements for radiation from H and N_2^+ for H^+ projectiles incident onto N_2. Thus, the initial and final states of both the projectile and target were determined. The energy range was 1.3–32 keV. At lower energies (<2 keV) several CTE measurements have been reported. Schlumbohm[8] obtained CTE data for Ne^+ projectiles with targets of N_2, O_2, and CO_2 for energies up to 250 eV. He found that the first negative system of N_2^+ was very strong, with a peak cross section at about 20 eV. Saban and Moran[9] also studied the $Ne^+ + N_2$ reaction and obtained the same maximum at 20 eV. The cross section then decreased to a minimum at 350 eV and was rising with increasing energy up through their maximum energy 450 eV. Salop, Lorents, and Peterson[10] made CTE measurements for He^+ and N_2^+ incident on alkali atoms at ion energies from 50–1600 eV. For He^+ they observed alkali ion radiation, while N_2^+ projectiles produced mainly radiation from the N_2 second positive system.

We have measured the fraction of the total emission which results from charge-transfer events in which the target ion is left in an excited state. This fraction, along with the total emission cross section, permits one to obtain the CTE cross section. In this paper we report the cross sections for emission of the 3914-Å radiation of the first negative N_2^+ band occurring in coincidence with electron transfer from the N_2^+ target molecules to energetic projectile ions. The projectile ions employed were H^+ and singly charged ions of each of the inert gases. The energy range covered was 10–100 keV. There are no published results to compare with our data obtained for the inert-gas ions. Our proton data are compared with that of Wehrenberg and Clark.[5]

II. APPARATUS AND EXPERIMENTAL PROCEDURE

The method employed in the present experiment was that used by Wehrenberg and Clark.[5] Delayed coincidences were detected between photons emitted from the ionized target molecules and the neutralized projectiles. Each pulse from the photon detector channel initiated a voltage ramp in a time-to-amplitude converter (TAC). The ramp was terminated by the arrival of a pulse from the neutral particle detector, so that a distribution in ramp amplitude was obtained corresponding to the distribution in delay time between the photons and neutralized projectiles. The amplitude distribution contained true coincidences and accidental coincidences, and it was necessary in the data reduction process to subtract the accidental from the total number of events. During the experiment it was also necessary to measure the integrated ion beam current, the pressure in the reaction region, and the integrated number of neutral particles resulting from charge transfer in the reaction region. These quantities, along with geometrical constants of the apparatus and the appropriate total charge-transfer cross section, permitted the determination of the fraction of the photons which resulted from CTE. It is necessary to know the total emission cross section to obtain the charge-transfer-emission cross section from this fraction.

Figure 1 shows a schematic drawing of the apparatus. The differentially pumped reaction chamber had an effective length of 2.63 cm. The pressure in this region was monitored by a capacitive manometer and was kept sufficiently low that single-collision conditions prevailed. The ion beam path in this chamber passed through the focal point of a quartz lens (not shown) having an f number of 1.6, which was mounted inside the reaction chamber. The light collected by this lens passed through a quartz window. A second quartz lens (not shown) formed an image on the photocathode of a C31034 (Ref. 11) photomultiplier tube. This tube has a small photocathode (6 mm × 10 mm) in order to reduce the dark current. A 3914-Å filter, having a band pass of 25 Å full width at half-maximum, was interposed in the light path between the window and the second lens. The output signal from the tube entered an amplifier-discriminator (time-pickoff unit), and the pulses thus obtained initiated ramps in the TAC unit.

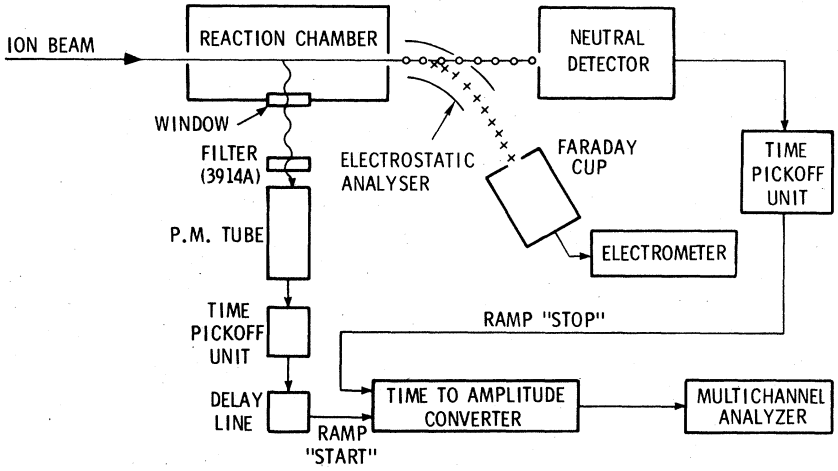

FIG. 1. Schematic drawing of the apparatus.

The ion beam was supplied by a 100-kV dc accelerator having a simple electron impact ion source. Since only a small beam current was required ($<10^{-10}$ A), the energy of the ionizing electrons could be kept low, so that the fraction of ions produced in excited states was negligible. The distance from the accelerator column to the experiment was 3.75 m, so that short-lived excited states had decayed before the ions arrived. The ions were passed through a magnetic analyzer which selected the appropriate ion species. A pair of electrostatic deflection plates, located just before the reaction cell, could be used to remove the ion beam for purposes of background correction, a process which will be discussed shortly. After passing through the reaction region, the residual ion beam was electrostatically deflected into a Faraday cup and the current integrated. The total beam charge incident onto the collision region was obtained from this integral by correcting for the fraction neutralized. The integration process minimized the effect of minor beam variations during the experiment.

The fast neutral atoms resulting from electron capture by projectile ions in the reaction region were transmitted through an aperture in the electrostatic analyzer and were incident on the cathode of an electron multiplier (neutral detector). The pulses from the multiplier were processed by an amplifier-discriminator (time-pickoff unit) identical to that used in the photon channel. The resulting pulses were transmitted to the TAC unit and served to terminate any voltage ramps in progress at their arrival. The distance from the center of the reaction region to the electron multiplier cathode was 28.9 cm so that the delay between the charge-transfer event and the arrival of the neutral atom ranged 66–1700 nsec for the ions and energies used. This range could be accommodated by a set of delay lines which could be inserted in the counting system.

It was noted that the function of the TAC unit was to convert time interval to amplitude. The distributions in ramp amplitude were accumulated in a multichannel analyzer. Figure 2 shows such a distribution, obtained for the case of 20-keV H^+

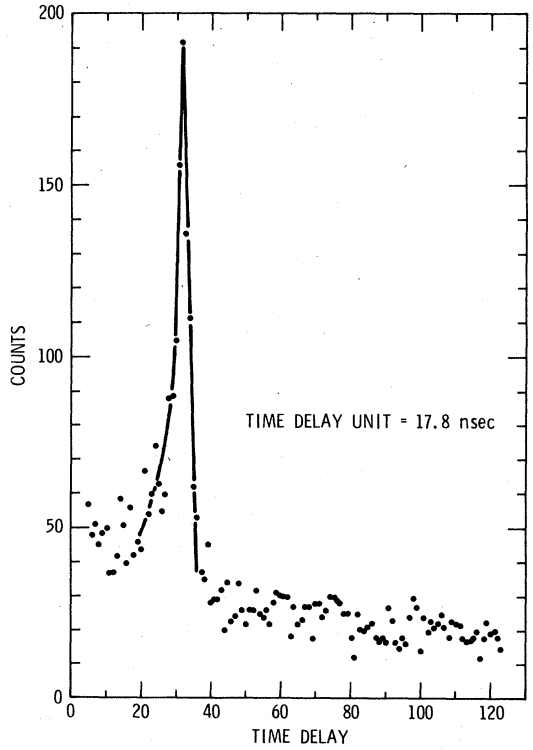

FIG. 2. Time-to-amplitude converter output versus delay time for 20-keV H^+ on N_2.

ions. It can be seen that the distribution has the shape of a peak superimposed on a decreasing background. The peak ends sharply at a time delay of about 570 nsec. This corresponds to the maximum delay between ramp initiation and termination and results from the prompt emission of a photon from CTE. Keeping in mind that the signal from the neutral atom always occurs at a fixed time after the CTE event for a given ion velocity, and the ramp is initiated by the photon emission, it follows that the smaller the time delay (channel number) the greater the delay in photon emission. If the delay in photon emission is sufficiently great, the delay limit is exceeded and there can be no coincidence unless delay is introduced into the neutral particle channel. Since the rate of photon emission decreases exponentially with time after excitation, the distribution should have a sharp peak at the maximum time and decrease exponentially as the channel number is decreased. Distributions made with delay per channel much smaller than the 17.8 nsec in Fig. 2 indicate that the distribution is exponential. The lifetime of the excited state can be obtained from the time constant of this exponential. Good agreement with the previously measured lifetime[12] of 59 nsec of the $B\,^2\Sigma$ state of N_2^+ was obtained.

The experimental procedure incorporated corrections for (a) a neutral component in the incident beam, (b) noise pulses from the photomultiplier tube, and (c) accidental coincidences. Each of these will now be discussed.

The incoming ion beam travels several meters after passing through the magnetic analyzer. Residual gas in this region can result in charge transfer, and the resulting neutral projectiles may be able to reach the electron multiplier. Without the correction, such neutrals would be treated as originating within the reaction cell, and the detector efficiency obtained would be too high. The fraction of photons from CTE would then be too low. To make the correction, the ion beam was removed by electrostatic deflection just prior to entrance into the reaction cell and the residual neutral beam was measured. Since there was little change in the pressure in the drift region when the pressure was varied in the reaction cell, a simple subtractive correction was made to the neutral rate observed during the coincidence run. This correction was generally less than 10%. The correction measurement was made several times during each data run and the results averaged.

The pulse rate due to noise in the photomultiplier was obtained by blocking the beam before the reaction region and determining the count rate due to dark current. This was measured several times during each data run, and the results averaged. The signal-to-noise ratio varied from about 0.4–8.4 depending on the projectile ion, its energy, and the pressure. To minimize this background, the photomultiplier tube was operated at a temperature of −40 °C.

To correct for the background of accidental coincidences in the ramp amplitude distribution, it was necessary to perform an analysis of the distribution in both the region in which true coincidences could occur and the region of time delays (channel numbers) so great that a true coincidence could not have occurred. This analysis involved five classes of events. These are (1) ramps initiated by either noise or by photons which are not the result of CTE and which are randomly terminated by neutral detector pulses; (2) ramps initiated by photons from CTE which are accidentally terminated before the correlated neutral arrives at the detector; (3) ramps initiated by CTE photons which were not terminated by the correlated neutral due to detector inefficiency but which were later terminated by an uncorrelated neutral; (4) ramps initiated by a CTE photon which occurred so late that the correlated neutral had already reached the detector, and which were then terminated by an uncorrelated neutral; and (5) true coincidences (CTE-photon-initiated ramps terminated by the correlated neutrals). The analysis showed that for channel number sufficiently large that there could be no true coincidences, the background decreased as a simple exponential with channel number with the decay constant equal to the neutral detection rate multiplied by the time duration of a channel. The analysis showed further that if this exponential background was extrapolated back through the true signal region and subtracted from the calculated signal (channel by channel) and the difference summed over all of the signal channels, then the result was just

$$N_0 = N_t \eta (1 - e^{-t_0/\tau}) e^{-t_1/\tau} .$$

Here N_0 is the number of observed coincidences (after background subtraction), N_t is the number of true CTE photons, η is the neutral detector efficiency, t_0 is the time over which true coincidences could have been obtained, t_1 is the minimum delay time in the measured distribution, and τ is the lifetime of the excited state. Typically 25 channels of possible true coincidences are utilized in the summing process. For a channel width of 17.8 nsec, as in Fig. 2, the exponential term involving t_0 is of the order of 10^{-3} and hence is quite negligible compared to unity. The background was obtained by fitting the first 40 channels following the end of the true coincidence distribution to an exponential decay. Correction was made for the

factor involving t_1.

The above procedure required the determination of the neutral detector efficiency for each data run. This in turn required knowledge of the value of the cross section for total charge transfer for each projectile at each energy used. These values were either obtained from previous measurement[13,14] or they were determined in auxiliary experiments. The latter cases will be noted in the results. The detector efficiency is the ratio of the number of neutrals counted to that which should have been obtained based on the integrated beam current, the collision length, the pressure, the total charge-transfer cross section, and assuming each incident neutral was detected. This efficiency depended on the secondary emission properties of the electron multiplier cathode, the projectile species and velocity, and the discriminator setting. Detector efficiency values in the vicinity of 0.5 were typical.

The length of a data run depended on the CTE cross section, the pressure in the reaction region, and the beam current. The pressure was limited to about 1 mTorr in order to satisfy the single-collision condition. The beam current maximum was limited by the allowable neutral counting rate. When this became too high, the accidental coincidence background became prohibitive. In most cases at least 10^3 true coincidences were obtained in the distribution and a run time of the order of 2×10^3 sec was usually sufficient for this. The neutral rate was low enough under these conditions so that there was no appreciable error due to pulse pileup in the neutral channel.

It was possible from the total photon count rate, the beam current, and the pressure to obtain relative measurements of the total emission cross sections. These could be normalized to our previous measurements in the case of H^+ projectiles[15] so that an internal consistency check could be made. This normalization also permitted the determination of the total emission cross sections for all other projectiles.

The uncertainty in the values obtained for the CTE cross sections varied because of the background subtraction process. In the extreme cases the statistical uncertainty in coincidence rate was as high as 10% and as low as 4%. Other major sources of error in determining the fraction of photons produced by CTE are the pressure measurement and the uncertainty in σ_{10}, the total charge-transfer cross section. Taking these to be 5% and 9%, respectively, we arrive at an uncertainty ranging 11–15% for the values given for the fraction f. The CTE cross section values have the additional uncertainty in the total emission cross sections. This is typically about 10%, so that the resulting errors in the CTE cross sections range 15–18%. Since these limits are not greatly different, we ascribe an error of ±17% to all of the cross sections obtained and ±13% to all of the fractions.

III. RESULTS

A. H^+ projectiles

In order to check the performance of the apparatus and the validity of the experimental procedure, we measured the CTE cross section as a function of energy for H^+ projectiles. Figure 3 shows our results along with those of Wehrenberg and Clark.[5] Over the range 10–65 keV, where the two data sets overlap, the agreement is excellent. The total charge-transfer cross section[13] is also shown over the entire energy range. The shapes are similar with the total charge-transfer cross section being about 20 times greater in magnitude.

It was noted previously that relative values for the total emission cross section could be obtained. These were normalized to give the best overall fit to the curve we obtained in a previous work.[15] Both sets of data are shown in Fig. 4. The agreement in energy dependence is quite satisfactory. Especially since the previous experiment employed both apparatus and method that were quite different from the present experiment.

By subtracting the CTE values from the total emission values (σ_E), we obtain indirectly the cross section (σ_{iE}) over the entire energy range for the alternative process of ionization with excitation. The results obtained are presented in Fig. 5. Along with this is shown the total ionization cross section of DeHeer *et al.*[16] There is again a similarity in shape with the total ionization cross section again being about 20 times greater in magnitude.

It is useful to be able to see the fraction (f) of the total emissions which result from the CTE. Figure 6 shows the dependence of f on energy. It is clear that the CTE is the dominant process at low energies but it decreases in importance as the energy increases.

B. Inert-gas ion projectiles

We have measured the cross sections for the CTE for all of the singly-ionized inert-gas projectiles. These are shown in Figs. 7–11. In each case we have also shown the total charge-transfer cross section and the fraction f. The value of f is nearly constant over the entire energy range for He^+, Ne^+, Ar^+, and Kr^+ and is between 0.6 and 1.0. The fraction is lower for Xe^+ and is more energy dependent. The CTE and total charge-transfer

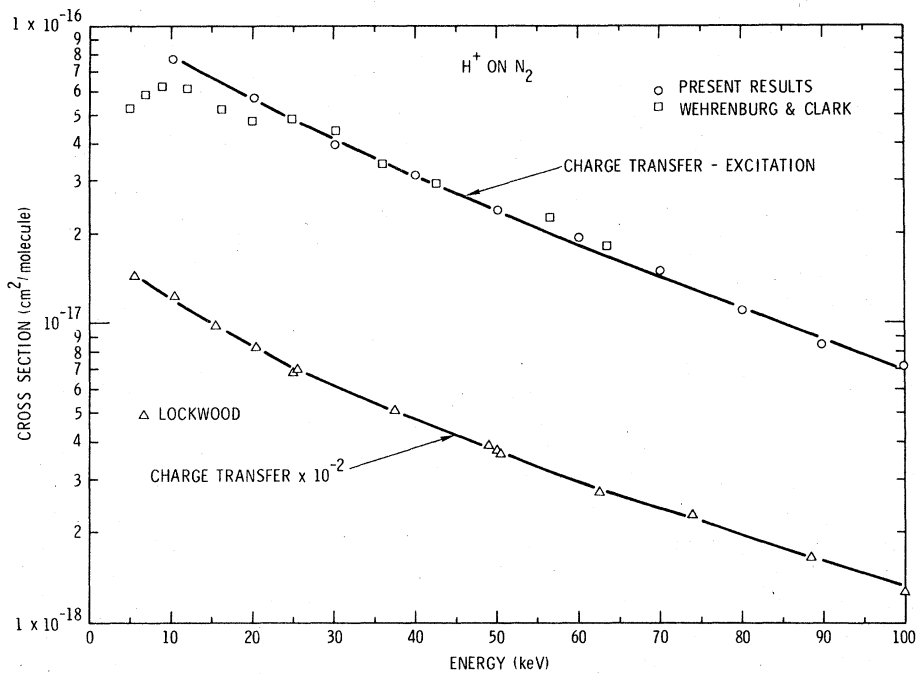

FIG. 3. Cross section for charge-transfer excitation and total charge transfer of H^+ on N_2 versus kinetic energy of the incident ion.

cross sections are similar in shape for He^+ and Ne^+, but dissimilar for the other three projectiles.

All of the results are summarized in Table II. In addition to the CTE cross sections and the values of the fraction f, the quantities $g = 1.41\sigma_{CTE}/\sigma_{10}$ (Ref. 17) and $\sigma_{iE} = \sigma_E - \sigma_{CTE}$ are also given. The quantity g is the fraction of all charge transfers leading to excitation of the $B\,^2\Sigma(v' = 0)$ state. Figures 12 and 13 show the graphs summarizing the values of f and g, respectively, for all of the projectiles used as a function of projectile velocity.

C. Auxiliary charge-transfer measurements

For most of the CTE measurements reported here the total charge-transfer cross sections σ_{10} were obtained from published data as previously noted. Nevertheless, some of the values were not available, and these were obtained during this investigation. The method and apparatus have been previously reported[13,14] and so will not be discussed here. The results obtained are presented in Table III.

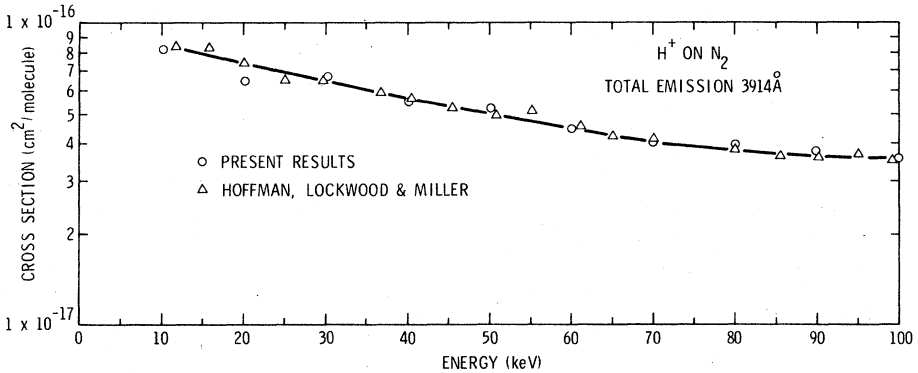

FIG. 4. Total cross section for emission of 3914-Å radiation for H^+ on N_2 versus kinetic energy of the incident ion.

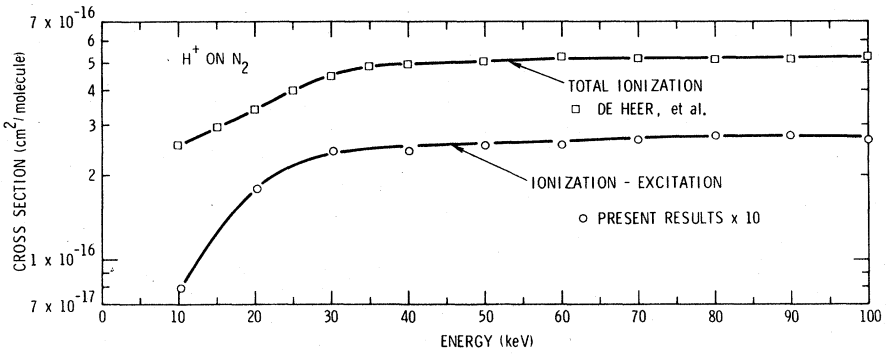

FIG. 5. Total cross section for ionization and ionization excitation for H^+ on N_2 versus kinetic energy of the incident ion.

IV. DISCUSSION

Even though there are no published experimental or theoretical results for the inert-gas ions to compare with the present data, some interesting comparisons can be made by examination of Fig. 12. First we can compare the values for the fraction f from Ne^+ and Ar^+ over the common velocity range. The algebraic signs of the ΔE's are different although the magnitudes are about the same (+2.81 and −2.99, respectively). Thus the reaction with Ne^+ is exothermic, while that with Ar^+ is endothermic. It will be noted that f is consistently greater for Ne^+ over this overlap region. A comparison can be made between He^+ and either Kr^+ or Xe^+. The reaction with He^+ (ΔE=+5.84) is exothermic, while the other two are endothermic. The magnitudes of ΔE for Kr^+ and Xe^+ (ΔE = −4.75 and −6.62, respectively) bracket that of He^+. It appears that the maximum value of f for He^+ is significantly greater than that of either Kr^+ or Xe^+. Thus it appears that in terms of the fraction of excitations produced by the charge-transfer process exothermic processes are more effective than endothermic ones.

A third observation can be made by comparing He^+ with Ne^+. These reactions are both exothermic, but He^+ has a greater ΔE and hence is further from energy resonance. It appears that f is greater for Ne^+, indicating that the magnitude of ΔE is also important. This is also indicated by the order in which the values of f occur in the

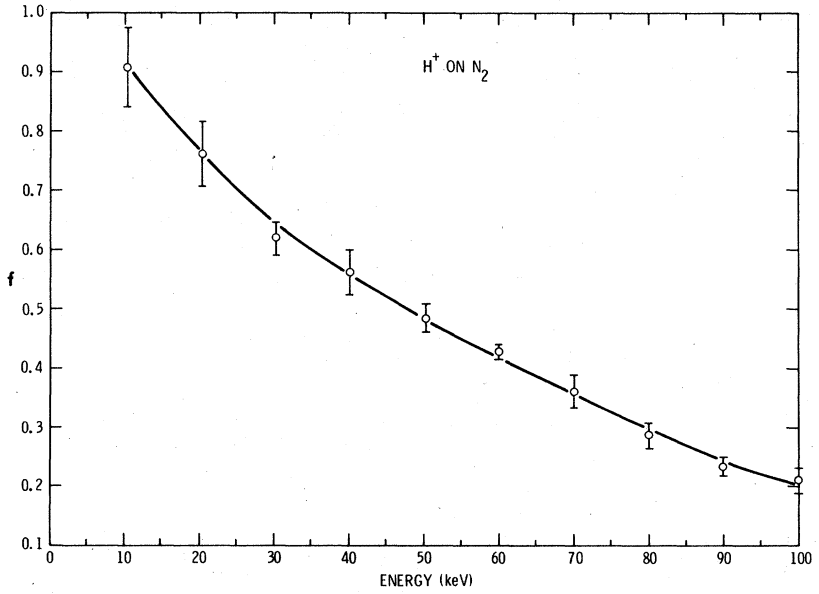

FIG. 6. Fraction f of the total emission which results from charge transfer for H^+ on N_2 versus kinetic energy of the incident ion.

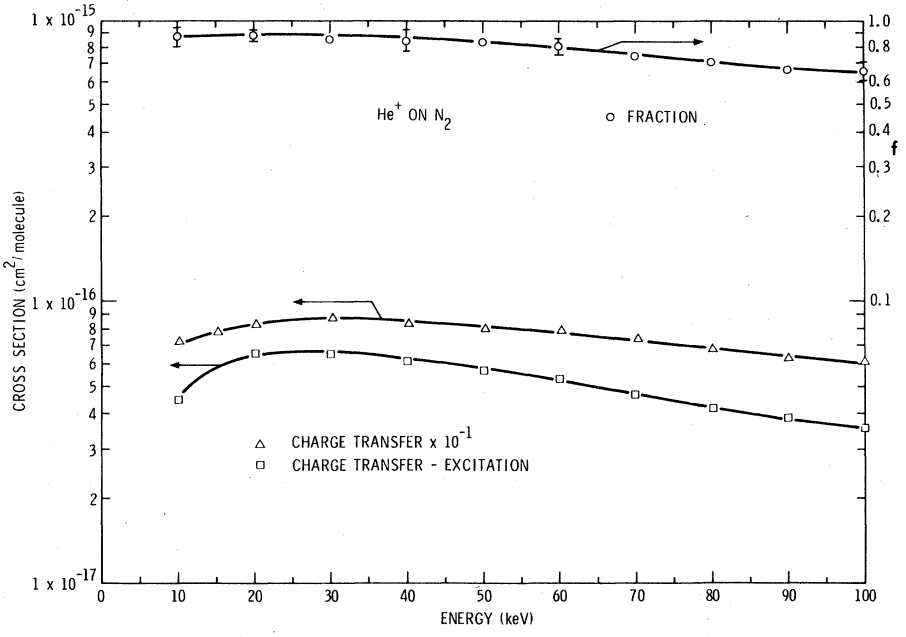

FIG. 7. Cross section for charge-transfer excitation and total charge transfer of He^+ on N_2 versus incident ion kinetic energy. Also shown is the fraction f of the total emission which results from charge transfer.

overlapping regions for Ar^+, Kr^+, and Xe^+, all of which are endothermic but with successively greater magnitudes of ΔE. The values of f decrease successively at the same velocity for this sequence. This may indicate that the velocity at which the maximum f occurs may increase with the magnitude of ΔE, in analogy with the adiabatic criterion.

The final observation to be made from the curves of Fig. 12 concerns H^+. The values of f produced in this case are as high as 0.9 at 10 keV and may go higher at lower energy. This might seem cur-

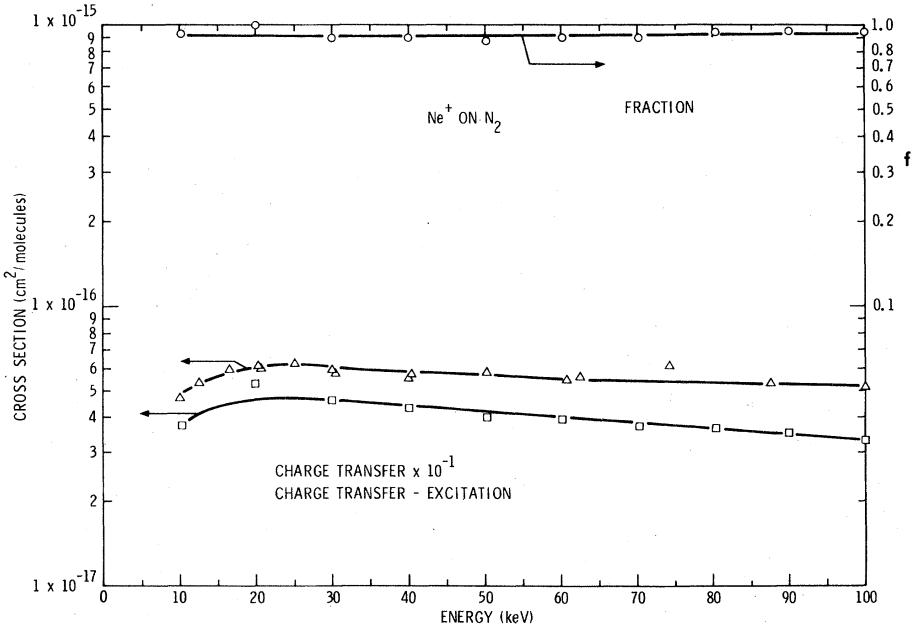

FIG. 8. Cross section for charge-transfer excitation and total charge transfer of Ne^+ on N_2 versus incident ion kinetic energy. Also shown is the fraction f of the total emission which results from charge transfer.

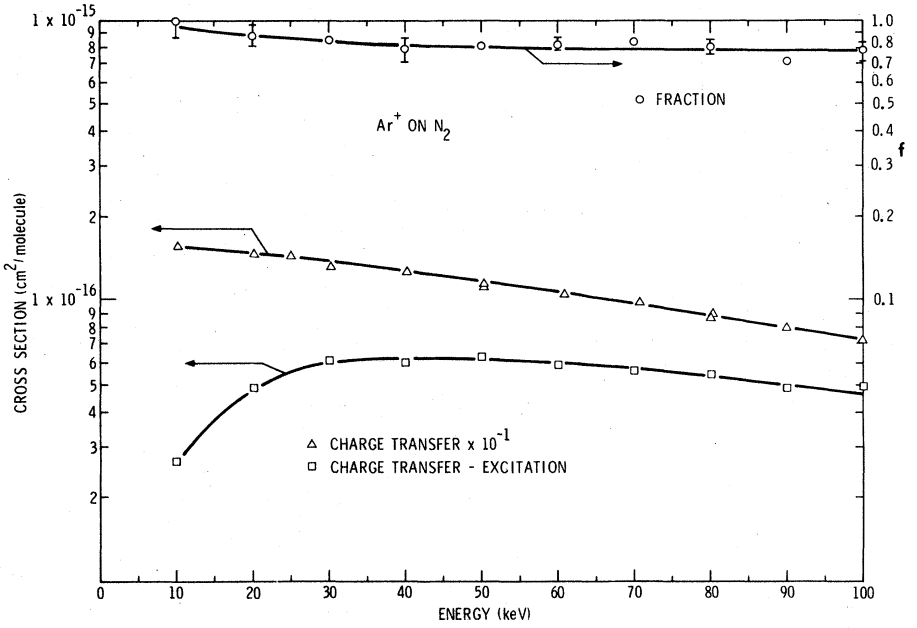

FIG. 9. Cross section for charge-transfer excitation and total charge transfer of Ar^+ on N_2 versus incident ion kinetic energy. Also shown is the fraction f of the total emission which results from charge transfer.

ious since the reaction is endothermic and the magnitude of ΔE is large ($\Delta E = -5.15$). However, unlike the inert-gas ions, H^+ can accept electrons of either spin and still produce H in the 1s ground state. In the case of the inert gases, half of the collisions would require transfer to a highly excited state on the basis of electron-spin considerations, with a correspondingly large endothermic energy defect. Thus one might expect that the cross sections and values of f for H^+ should be

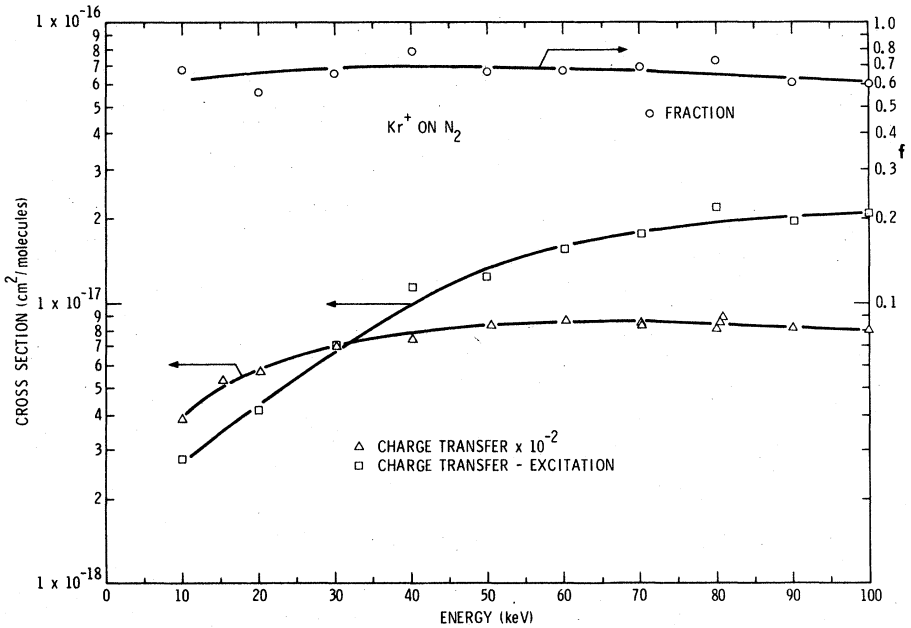

FIG. 10. Cross section for charge-transfer excitation and total charge transfer of Kr^+ on N_2 versus incident ion kinetic energy. Also shown is the fraction f of the total emission which results from charge transfer.

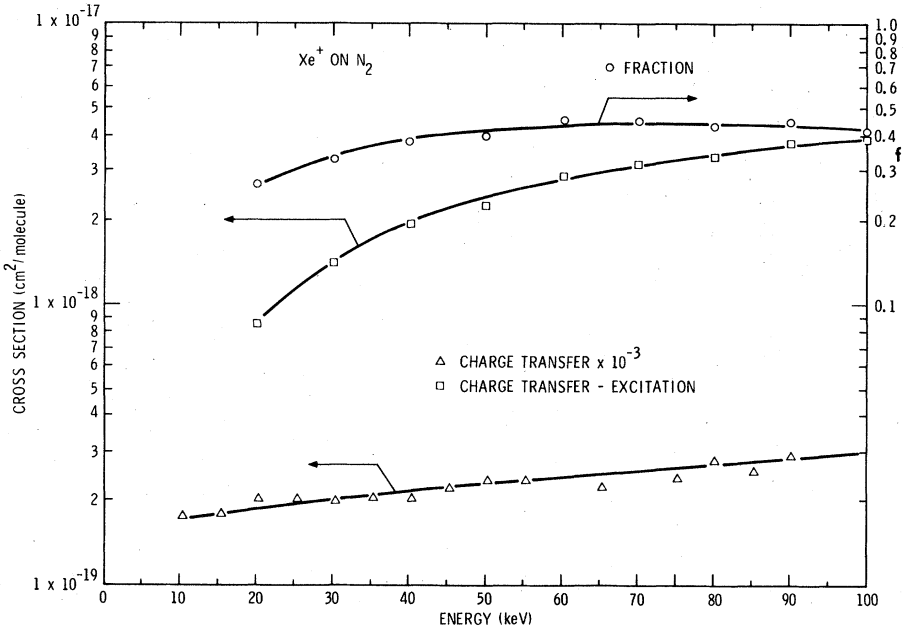

FIG. 11. Cross section for charge-transfer excitation and total charge transfer of Xe^+ on N_2 versus incident ion kinetic energy. Also shown is the fraction f of the total emission which results from charge transfer.

divided by a number approaching two if a comparison is to be made with inert-gas ions. This would reduce the H^+ values well below those of He^+, which has about the same ΔE but is exothermic.

It is difficult to draw many inferences from Fig. 13. Only He^+ exhibits a clear maximum in the value of g in the velocity ranges covered. H^+ and Ne^+ may have maxima in these data, but the uncertainties are too great to make this determination. Considering the shapes which exist in the limited velocity ranges, it appears that the peak occurs at lower velocity for exothermic reactions than for endothermic reactions having the same absolute ΔE. The Ne-Ar combination is a case in point. The remark made above concerning the magnitude of f for H^+ is also appropriate concerning the values of g.

Owing to the large uncertainties in the derived values of σ_{iE}, we shall not attempt to make comments about the values obtained. It is sufficient to say that the shapes show no substantial irregu-

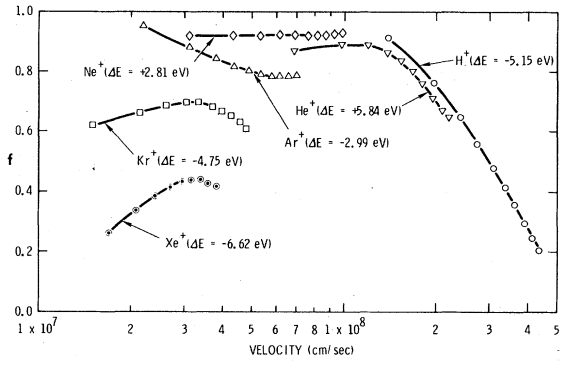

FIG. 12. Fraction f of the total emission which results from charge transfer for all ions studied on N_2 versus velocity of the incident ion. Also listed is the energy defect ΔE for charge-transfer excitation for each incident ion.

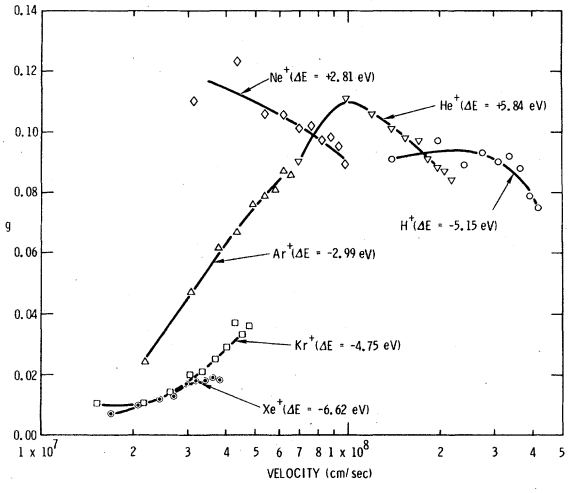

FIG. 13. The quantity $g=1.41\sigma_{CTE}/\sigma_{10}$ for all ions studied versus velocity of the incident ion. Also listed is the energy defect ΔE for charge-transfer excitation for each incident ion.

TABLE II. Summary of the charge-transfer-excitation cross sections and related quantities.

Projectile	Energy (keV)	Velocity (10^8 cm/sec)	σ_{CTE} (10^{-17} cm^2)	$f=\frac{\sigma_{CTE}}{\sigma_E}$	$g=\frac{1.41\sigma_{CTE}}{\sigma_{10}}$	$\sigma_{iE}=\sigma_E-\sigma_{CTE}$ (10^{-17} cm^2)
H^+	10.3	1.40	7.71	0.91	0.091	0.8
	20.3	1.97	5.71	0.76	0.097	1.8
	30.2	2.40	3.93	0.62	0.089	2.4
	40.1	2.77	3.13	0.56	0.093	2.4
	50.2	3.10	2.40	0.49	0.090	2.6
	60.1	3.39	1.93	0.43	0.092	2.6
	70.1	3.66	1.50	0.36	0.088	2.7
	80.1	3.92	1.10	0.29	0.079	2.8
	89.8	4.15	0.85	0.24	0.075	2.8
	100.0	4.38	0.72	0.21	0.076	2.7
He^+	10.0	0.692	4.47	0.87	0.090	0.6
	20.0	0.979	6.56	0.88	0.111	0.9
	30.0	1.20	6.51	0.85	0.106	1.1
	40.1	1.39	6.10	0.85	0.101	1.1
	50.0	1.55	5.70	0.84	0.098	1.1
	60.0	1.69	5.32	0.81	0.097	1.3
	70.1	1.83	4.64	0.74	0.091	1.6
	80.0	1.96	4.18	0.71	0.088	1.7
	90.1	2.08	3.87	0.67	0.087	1.9
	100.0	2.19	3.59	0.66	0.084	1.8
Ne^+	10.2	0.313	3.75	0.93	0.110	0.3
	20.0	0.438	5.31	1.00	0.123	
	30.0	0.536	4.58	0.90	0.106	0.5
	40.0	0.619	4.36	0.90	0.106	0.5
	50.3	0.694	4.03	0.88	0.101	0.6
	60.3	0.760	3.96	0.91	0.102	0.4
	70.2	0.820	3.71	0.90	0.097	0.4
	80.3	0.877	3.67	0.94	0.098	0.2
	90.1	0.929	3.53	0.95	0.095	0.2
	100.1	0.979	3.30	0.94	0.089	0.2
Ar^+	10.0	0.219	2.67	1.00	0.024	
	20.0	0.309	4.90	0.88	0.047	0.7
	30.1	0.380	6.11	0.85	0.062	1.1
	40.1	0.438	6.06	0.79	0.067	1.6
	50.0	0.489	6.32	0.82	0.076	1.4
	60.0	0.536	5.93	0.83	0.079	1.3
	70.0	0.579	5.65	0.85	0.081	1.0
	80.1	0.619	5.48	0.81	0.087	1.3
	90.1	0.657	4.88	0.72	0.086	2.0
	100.1	0.692	4.93	0.78	0.095	1.4
Kr^+	10.0	0.151	0.28	0.69	0.010	0.1
	20.0	0.213	0.42	0.57	0.010	0.3
	30.2	0.262	0.71	0.67	0.014	0.4
	40.2	0.303	1.14	0.79	0.020	0.3
	49.9	0.337	1.22	0.67	0.021	0.6
	60.1	0.370	1.55	0.67	0.025	0.8
	70.2	0.400	1.76	0.69	0.029	0.8
	80.0	0.427	2.19	0.73	0.037	0.8
	90.1	0.453	1.93	0.61	0.033	1.3
	99.9	0.477	2.04	0.60	0.036	1.4
Xe^+	20.0	0.170	0.09	0.27	0.007	0.2
	30.0	0.209	0.14	0.33	0.010	0.3
	40.0	0.241	0.19	0.38	0.012	0.3
	50.1	0.270	0.22	0.40	0.013	0.3
	60.2	0.296	0.29	0.46	0.017	0.3
	70.1	0.319	0.32	0.45	0.018	0.4
	80.0	0.341	0.34	0.43	0.018	0.4
	90.0	0.361	0.38	0.45	0.019	0.5
	99.8	0.381	0.38	0.41	0.018	0.6

TABLE III. Total charge-transfer cross section for inert-gas ions in N_2.[a-c]

He^+ Kinetic energy (keV)	σ_{10}	Ar^+ Kinetic energy (keV)	σ_{10}	Kr^+ Kinetic energy (keV)	σ_{10}	Xe^+ Kinetic energy (keV)	σ_{10}
80.0	6.73	80.0	8.61	10.0	3.89	80.0	2.78
90.0	6.32	90.1	8.03	80.0	8.06	90.1	2.88
99.6	6.02	99.8	7.34	90.1	8.10	100.0	3.05
				100.3	7.86		

[a]Units of σ_{10} are 10^{-16} cm^2/molecule.
[b]Data tabulated are for ground-state incident ions produced in an electron-impact source.
[c]Experimental uncertainty in σ_{10} is ± 9%.

larities. A lack of ionization data prevents any comparison of the ionization-excitation process with simple ionization, except in the case of H^+. Our data indicate that the two processes in this case have very nearly the same energy dependence with about 0.05 of the ionizing events leading to excitation.

ACKNOWLEDGMENTS

It is a pleasure for the authors to acknowledge the assistance of L. E. Ruggles throughout the conduct of this research. This work was supported by the United States Department of Energy.

[1]Ionization and excitation energy values (rounded to two decimal places) used herein are from Nat. Stand. Ref. Data Ser. Nat. Bur. Stand. 26 (1969).
[2]H. S. W. Massey, Rep. Prog. Phys. 12, 248 (1949).
[3]For a comprehensive review of the work up to 1972, see E. W. Thomas, *Excitation in Heavy Particle Collisions* (Wiley Interscience, New York, 1972).
[4]J. M. Hoffman, G. J. Lockwood, and G. H. Miller, Phys. Rev. A 9, 187 (1974).
[5]P. J. Wehrenberg and K. C. Clark, Phys. Rev. A 8, 173 (1973).
[6]F. J. DeHeer and J. F. M. Aarts, Physica (Utrecht) 48, 620 (1970).
[7]S. J. Young, J. S. Murray, and J. R. Sheridan, Phys. Rev. 178, 40 (1969).
[8]H. Schlumbohm, Z. Naturforsch. 23a, 1386 (1968).
[9]G. H. Saban and T. F. Moran, J. Chem. Phys. 57, 895 (1972).
[10]A. Salop, D. C. Lorents, and J. R. Peterson, J. Chem. Phys. 54, 1187 (1971).
[11]Manufactured by RCA.
[12]R. Anderson, At. Data 3, 227 (1975).
[13]G. J. Lockwood, Phys. Rev. 187, 161 (1969).
[14]G. J. Lockwood, Phys. Rev. A 2, 1406 (1970).
[15]J. M. Hoffman, G. J. Lockwood, and G. H. Miller, Phys. Rev. A 11, 841 (1975).
[16]F. J. DeHeer, J. Schutten, and H. Moustafa, Physica (Utrecht) 32, 1766 (1966).
[17]The excitation cross section is found by summing the emission cross sections for the various values of v''. Multiplication of the emission cross section for the (0,0) transition by 1.41 is equivalent to this process. B. N. Srivastava and I. M. Merza, Phys. Rev. 176, 137 (1968) provide a compilation of measurements and calculations of the relative probabilities for the (0,0), (0,1), and (0,2) transitions. The average of these adjusted for the very small probability for the (0,3) transition results in the factor of 1.41.